Communications in Nonlinear Science and Numerical Simulation 107 (2022) 106125

Contents lists available at ScienceDirect

Communications in Nonlinear Science and Numerical Simulation

journal homepage: www.elsevier.com/locate/cnsns

Virtual element method for a frictional contact problem with normal compliance

Bangmin Wu [a], Fei Wang [a,*,1], Weimin Han [b,2]

[a] School of Mathematics and Statistics, Xi'an Jiaotong University, Xi'an, Shaanxi 710049, China
[b] Department of Mathematics & Program in Applied Mathematical and Computational Sciences, University of Iowa, Iowa City, IA 52242, USA

ARTICLE INFO

Article history:
Available online 27 November 2021

MSC:
65N30
49J40

Keywords:
Virtual element method
Quasi-variational inequality
Coulomb's law of dry friction
Error estimate

ABSTRACT

We consider an elastostatic frictional contact problem with a normal compliance condition and Coulomb's law of dry friction, which can be modeled by a quasi-variational inequality. As a generalization of the finite element method, the virtual element method (VEM) can handle general polygonal meshes with hanging nodes, which are very suitable for solving problems with complex geometries or applying adaptive mesh refinement strategy. In this paper, we study the VEM for solving the frictional contact problem with the normal compliance condition. Existence and uniqueness results are obtained for the discretized scheme. Furthermore, a priori error analysis is established, and an optimal order error bound is derived for the lowest order virtual element method. One numerical example is given to show the efficiency of the method and to illustrate the theoretical error estimate.

© 2021 Elsevier B.V. All rights reserved.

1. Introduction

Processes of frictional contact between deformable bodies or between a deformable body and a rigid foundation are commonly seen in the industry and daily life. A considerable effort has been made on modeling and numerical analysis of the frictional contact problems. In this paper, we consider the numerical solution of a contact problem that describes the contact between a linearly elastic body and a deformable foundation, with the normal compliance condition and Coulomb's law of dry friction on the contact boundary. The contact problem is highly nonlinear, and its weak formulation is quasi-variational inequality. Solution existence and uniqueness for the quasi-variational inequality can be established by using the fixed point argument [1,2]. We note that inverse problems for nonlinear quasi-variational inequalities have been studied in [3,4]; finite element methods have been applied for solving quasi-variational inequalities, and a priori error estimates can be found in [5–8]. Recently, in [9], several discontinuous Galerkin methods with linear elements are introduced for solving a frictional contact problem with normal compliance, and a priori error estimates are established in [10]. Nitsche-type methods can be introduced for solving contact problems in the form of variational inequalities, e.g., [11–13].

It is known that the conforming finite element method cannot handle general polygonal meshes. To overcome this difficulty, the virtual element method (VEM) is proposed in [14], and its elemental level function space contains both

* Corresponding author.
E-mail addresses: wbmlll123456@stu.xjtu.edu.cn (B. Wu), feiwang.xjtu@xjtu.edu.cn (F. Wang), weimin-han@uiowa.edu (W. Han).

1 The work of this author was partially supported by the National Natural Science Foundation of China (Grant No. 12171383).
2 The work of this author was partially supported by Simons Foundation Collaboration Grants, No. 850737.

https://doi.org/10.1016/j.cnsns.2021.106125
1007-5704/© 2021 Elsevier B.V. All rights reserved.

polynomials and non-polynomial functions. The method has advantages in handling very general (including non-convex) polygonal elements, so we can solve problems on complex geometries with ease. Through the introduction of a projection operator from a virtual element space to a polynomial space, the stiffness matrix can be formed without actually computing the non-polynomial functions. The method has been applied to solve a variety of scientific and engineering problems [15–20]. In particular, it has been applied to solve variational inequalities. In [21], the virtual element method is applied to solve a two-body contact problem, but no error estimate is derived. The VEM is applied to solve the obstacle problem and simplified friction problem in [22,23], respectively, and a priori error analysis is established. The VEM is studied for a frictional contact problem in [24]. In [25,26], the VEM is developed and analyzed for solving elliptic hemivariational inequalities with applications to contact mechanics. In [27], a general framework is established to study the conforming and nonconforming virtual element methods for solving a Kirchhoff plate contact problem with friction, and a priori error estimates are derived. The nonconforming VEM is studied to solve a hemivariational inequality for the stationary Stokes equations with a nonlinear slip boundary condition in [28]. In this paper, we construct and analyze the virtual element method for a frictional contact problem with normal compliance. Under some reasonable assumptions, existence and uniqueness results are proved for the VEM scheme. Error estimates are derived for the numerical solution, and an optimal convergence order is obtained for the lowest-order virtual element. Furthermore, numerical results show that the VEM scheme works well on general polygonal elements.

The rest of the paper is organized as follows. In Section 2, we introduce the frictional contact problem with normal compliance, and present its weak formulation as a quasi-variational inequality. In Section 3, we give the virtual element method scheme for the problem. In Section 4, we derive an a priori error estimate, which is of optimal order for the lowest order element. In Section 5, computer simulation results are reported to provide numerical evidence of the theoretically predicted optimal convergence order.

2. A frictional contact problem with normal compliance

In this section, we introduce an elastostatic contact problem, which is modeled with the normal compliance condition and Coulomb's law of dry friction. Then we present the weak formulation of the problem.

2.1. Contact problem

Let $\Omega \subset \mathbb{R}^d$ $(d = 2, 3)$ be an open bounded connected domain with a Lipschitz boundary Γ that is divided into three parts $\overline{\Gamma_D}$, $\overline{\Gamma_F}$ and $\overline{\Gamma_C}$ with Γ_D, Γ_F and Γ_C relatively open and mutually disjoint such that meas$(\Gamma_D) > 0$. The displacement $\boldsymbol{u} : \Omega \subset \mathbb{R}^d \to \mathbb{R}^d$ is a vector-valued function. The linearized strain tensor is $\boldsymbol{\varepsilon}(\boldsymbol{u}) = \frac{1}{2}(\nabla \boldsymbol{u} + (\nabla \boldsymbol{u})^t)$. The symbol $\mathbb{S}^d$ denotes the space of 2nd-order symmetric tensors on $\mathbb{R}^d$ with the inner product $\boldsymbol{\sigma} : \boldsymbol{\tau} = \sigma_{ij}\tau_{ij}$. Throughout the paper, we adopt the summation convention over repeated indices, e.g., $\sigma_{ij}\tau_{ij}$ stands for $\sum_{i,j=1}^{d} \sigma_{ij}\tau_{ij}$. Let $\boldsymbol{\nu}$ be the unit outward normal to Γ. For a vector $\boldsymbol{v}$ defined on the boundary, denote its normal component and tangential component by $v_\nu = \boldsymbol{v} \cdot \boldsymbol{\nu}$ and $\boldsymbol{v}_\tau = \boldsymbol{v} - v_\nu \boldsymbol{\nu}$ on the boundary. Similarly, for a tensor-valued function $\boldsymbol{\sigma} : \Omega \to \mathbb{S}^d$, we denote its normal component $\sigma_\nu = (\boldsymbol{\sigma}\boldsymbol{\nu}) \cdot \boldsymbol{\nu}$ and tangential part $\boldsymbol{\sigma}_\tau = \boldsymbol{\sigma}\boldsymbol{\nu} - \sigma_\nu \boldsymbol{\nu}$. Then, we have

$$(\boldsymbol{\sigma}\boldsymbol{\nu}) \cdot \boldsymbol{v} = (\sigma_\nu \boldsymbol{\nu} + \boldsymbol{\sigma}_\tau) \cdot (v_\nu \boldsymbol{\nu} + \boldsymbol{v}_\tau) = \sigma_\nu v_\nu + \boldsymbol{\sigma}_\tau \cdot \boldsymbol{v}_\tau.$$

For a tensor-valued function $\boldsymbol{\sigma}$, define its divergence by $\operatorname{div}\boldsymbol{\sigma} = (\partial_j \sigma_{ij})_{1\le i\le d}$. Then, for any symmetric tensor $\boldsymbol{\sigma}$ and any vector field $\boldsymbol{v}$, both are sufficiently smooth, we have the following integration by parts formula

$$\int_\Omega \operatorname{div}\boldsymbol{\sigma} \cdot \boldsymbol{v}\, dx = \int_\Gamma \boldsymbol{\sigma}\boldsymbol{\nu} \cdot \boldsymbol{v}\, ds - \int_\Omega \boldsymbol{\sigma} : \boldsymbol{\varepsilon}(\boldsymbol{v})\, dx. \tag{2.1}$$

We consider a static contact problem with a deformable foundation for the deformation of a linearly elastic body occupying the domain Ω. Following [1,2,9], the pointwise formulation of the contact problem is to find a displacement field $\boldsymbol{u}$ and a stress field $\boldsymbol{\sigma}$ such that

$$\boldsymbol{\sigma} = \mathcal{C}\boldsymbol{\varepsilon}(\boldsymbol{u}) \quad \text{in } \Omega, \tag{2.2}$$

$$-\operatorname{div}\boldsymbol{\sigma} = \boldsymbol{f}_1 \quad \text{in } \Omega, \tag{2.3}$$

$$\boldsymbol{u} = \boldsymbol{0} \quad \text{on } \Gamma_D, \tag{2.4}$$

$$\boldsymbol{\sigma}\boldsymbol{\nu} = \boldsymbol{f}_2 \quad \text{on } \Gamma_F, \tag{2.5}$$

$$-\sigma_\nu = p_\nu(u_\nu - g_a) \quad \text{on } \Gamma_C, \tag{2.6}$$

$$|\boldsymbol{\sigma}_\tau| \le p_\tau(u_\nu - g_a) \quad \text{on } \Gamma_C, \tag{2.7}$$

$$\boldsymbol{\sigma}_\tau = -p_\tau(u_\nu - g_a)\,\boldsymbol{u}_\tau/|\boldsymbol{u}_\tau| \quad \text{if } \boldsymbol{u}_\tau \ne \boldsymbol{0} \text{ on } \Gamma_C, \tag{2.8}$$

$$|\boldsymbol{\sigma}_\tau| < p_\tau(u_\nu - g_a) \quad \Rightarrow \quad \boldsymbol{u}_\tau = \boldsymbol{0} \quad \text{on } \Gamma_C. \tag{2.9}$$

Here, (2.2) represents the constitutive law of the linearly elastic material, and we assume the bounded, symmetric and positive definite elasticity tensor $\mathcal{C}$ is constant. (2.3) is the equilibrium equation in Ω under volume forces of density

$\boldsymbol{f}_1 \in [L^2(\Omega)]^d$. Dirichlet boundary condition (2.4) implies that the elastic body is clamped on Γ_D, and Neumann boundary condition (2.5) means that surface tractions of density $\boldsymbol{f}_2 \in [L^2(\Gamma_F)]^d$ act on Γ_F. The function g_a denotes the initial gap between the body and the deformable foundation. On contact boundary Γ_C, the normal compliance condition (2.6) depicts that the reactive normal pressure depends on penetration of the elastic body in the foundation. The Coulomb's law of dry friction is described by relations (2.7)–(2.9), which states that the magnitude of the shear stress $\boldsymbol{\sigma}_\tau$ cannot exceed the maximum frictional resistance $p_\tau(u_\nu - g_a)$. There is no relative sliding between the body and the foundation when the magnitude of $\boldsymbol{\sigma}_\tau$ is less than the upper bound $p_\tau(u_\nu - g_a)$; relative sliding may occur when the magnitude of $\boldsymbol{\sigma}_\tau$ reaches the critical value $p_\tau(u_\nu - g_a)$, and in that case, the direction of $\boldsymbol{\sigma}_\tau$ is opposite to that of $\boldsymbol{u}_\tau$. For the functions p_e $(e = \nu, \tau)$, we assume

$$\begin{cases} (a)\, p_e : \Gamma_C \times \mathbb{R} \to \mathbb{R}_+; \\ (b)\, \text{there exists } L_e > 0, \text{ s.t. } |p_e(\boldsymbol{x}, r_1) - p_e(\boldsymbol{x}, r_2)| \le L_e |r_1 - r_2| \\ \qquad\qquad\qquad\qquad\qquad \forall\, r_1, r_2 \in \mathbb{R},\ \text{a.e. } \boldsymbol{x} \in \Gamma_C; \\ (c)\, \text{the mapping } \boldsymbol{x} \mapsto p_e(\boldsymbol{x}, r) \text{ is measurable on } \Gamma_C \text{ for any } r \in \mathbb{R}; \\ (d)\, p_e(\boldsymbol{x}, r) = 0 \quad \forall\, r \le 0,\ \text{a.e. } \boldsymbol{x} \in \Gamma_C. \end{cases} \tag{2.10}$$

The gap function satisfies

$$g_a \in L^2(\Gamma_C), \quad g_a(\boldsymbol{x}) \ge 0 \text{ a.e. } \boldsymbol{x} \in \Gamma_C. \tag{2.11}$$

In what follows, c denotes a positive constant independent of mesh-size, which may take different values at different occurrences.

2.2. Weak formulation

The contact problem will be studied through its weak formulation. For this purpose, we define a function space

$$\boldsymbol{V} = \left\{ \boldsymbol{v} \in [H^1(\Omega)]^d : \boldsymbol{v}|_{\Gamma_D} = \boldsymbol{0} \right\}$$

for the displacement field. Since meas$(\Gamma_D) > 0$, Korn's inequality holds (cf. [29, p. 79]): for some constant $c > 0$ depending only on Ω and Γ_D such that

$$\|\boldsymbol{v}\|_{[H^1(\Omega)]^d} \le c \int_\Omega \boldsymbol{\varepsilon}(\boldsymbol{v}) : \boldsymbol{\varepsilon}(\boldsymbol{v})\, dx \quad \forall\, \boldsymbol{v} \in \boldsymbol{V}. \tag{2.12}$$

Consequently, $\boldsymbol{V}$ is a Hilbert space with the norm defined by the relation

$$\|\boldsymbol{v}\|_{\boldsymbol{V}}^2 := \int_\Omega \boldsymbol{\varepsilon}(\boldsymbol{v}) : \boldsymbol{\varepsilon}(\boldsymbol{v})\, dx \quad \forall\, \boldsymbol{v} \in \boldsymbol{V},$$

and the norm $\|\cdot\|_{\boldsymbol{V}}$ is equivalent to the standard norm $\|\cdot\|_{[H^1(\Omega)]^d}$ over $\boldsymbol{V}$. By a standard approach, the following weak formulation can be derived for the contact problem (2.2)–(2.9) [2]:

Problem (P). Find a displacement field $\boldsymbol{u} \in \boldsymbol{V}$ such that

$$a(\boldsymbol{u}, \boldsymbol{v} - \boldsymbol{u}) + j(\boldsymbol{u}, \boldsymbol{v}) - j(\boldsymbol{u}, \boldsymbol{u}) \ge (\boldsymbol{f}, \boldsymbol{v} - \boldsymbol{u}) \quad \forall\, \boldsymbol{v} \in \boldsymbol{V}, \tag{2.13}$$

where

$$a(\boldsymbol{u}, \boldsymbol{v}) = \int_\Omega \mathcal{C}\boldsymbol{\varepsilon}(\boldsymbol{u}) : \boldsymbol{\varepsilon}(\boldsymbol{v})\, dx \quad \forall\, \boldsymbol{u}, \boldsymbol{v} \in \boldsymbol{V},$$

$$(\boldsymbol{f}, \boldsymbol{v}) = \int_\Omega \boldsymbol{f}_1 \cdot \boldsymbol{v}\, dx + \int_{\Gamma_F} \boldsymbol{f}_2 \cdot \boldsymbol{v}\, ds \quad \forall\, \boldsymbol{v} \in \boldsymbol{V}, \tag{2.14}$$

and

$$j(\boldsymbol{u}, \boldsymbol{v}) = j_\nu(\boldsymbol{u}, \boldsymbol{v}) + j_\tau(\boldsymbol{u}, \boldsymbol{v}) \quad \forall\, \boldsymbol{u}, \boldsymbol{v} \in \boldsymbol{V}. \tag{2.15}$$

Here,

$$j_\nu(\boldsymbol{u}, \boldsymbol{v}) = \int_{\Gamma_C} p_\nu(u_\nu - g_a) v_\nu\, ds,$$
$$j_\tau(\boldsymbol{u}, \boldsymbol{v}) = \int_{\Gamma_C} p_\tau(u_\nu - g_a) |\boldsymbol{v}_\tau|\, ds.$$

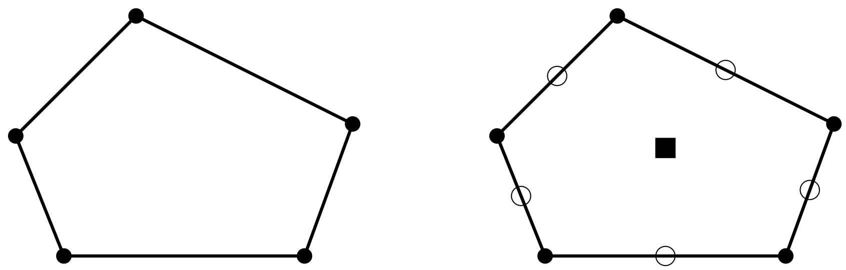

Fig. 1. Local degrees of freedom of $\boldsymbol{V}_h^K$ for $k = 1$ (left) and $k = 2$ (right).

Note that the functional j depends on u_ν, so the problem is highly nonlinear. By the assumption (2.10), we can get the following inequality (Theorem 5.38 in [2])

$$j(\boldsymbol{u}_1, \boldsymbol{v}_2) - j(\boldsymbol{u}_1, \boldsymbol{v}_1) + j(\boldsymbol{u}_2, \boldsymbol{v}_1) - j(\boldsymbol{u}_2, \boldsymbol{v}_2) \\ \le (L_\nu + L_\tau)\|\boldsymbol{u}_1 - \boldsymbol{u}_2\|_{L^2(\Gamma_C)}\|\boldsymbol{v}_1 - \boldsymbol{v}_2\|_{L^2(\Gamma_C)} \quad \forall\, \boldsymbol{u}_1, \boldsymbol{u}_2, \boldsymbol{v}_1, \boldsymbol{v}_2 \in \boldsymbol{V}. \tag{2.16}$$

Because the elasticity tensor is bounded and positive definite, we see that there exist two constants, $m > 0$ and $M > 0$, depending on some parameters raised in $\mathcal{C}$, such that

$$m\|\boldsymbol{v}\|_{\boldsymbol{V}}^2 \le a(\boldsymbol{v}, \boldsymbol{v}) \le M\|\boldsymbol{v}\|_{\boldsymbol{V}}^2. \tag{2.17}$$

By the trace theorem, there exists a positive constant c_3, depending only on Ω, such that

$$\|\boldsymbol{v}\|_{[L^2(\Gamma)]^d} \le c_3\|\boldsymbol{v}\|_{[H^1(\Omega)]^d} \quad \forall\, \boldsymbol{v} \in [L^2(\Gamma)]^d. \tag{2.18}$$

Combining (2.12) and (2.18), there exists a constant $C_0 > 0$, such that

$$\|\boldsymbol{v}\|_{L^2(\Gamma_C)^d} \le C_0\|\boldsymbol{v}\|_{\boldsymbol{V}} \quad \forall\, \boldsymbol{v} \in \boldsymbol{V}. \tag{2.19}$$

Under the assumptions (2.10)–(2.11) and the smallness condition $C_0^2(L_\nu+L_\tau) < m$, for any $\boldsymbol{f}_1 \in [L^2(\Omega)]^d$ and $\boldsymbol{f}_2 \in [L^2(\Gamma_F)]^d$, the quasi-variational inequality (2.13) has a unique solution [1,2].

3. Virtual element method

In this section, we introduce a virtual element method to solve Problem (P). For simplicity, we only consider the case where Ω is a two-dimensional polygonal domain.

We begin with a family of decompositions $\{\mathcal{T}_h\}_h$ of $\overline{\Omega}$ into polygonal elements denoted by K. Let $h_K = \operatorname{diam}(K)$ and $h = \max\{h_K : K \in \mathcal{T}_h\}$. All the subdivisions are compatible with the boundary splitting: $\Gamma = \overline{\Gamma_D} \cup \overline{\Gamma_F} \cup \overline{\Gamma_C}$. Furthermore, we assume that Γ_C is split as $\Gamma_C = \cup_{1\le i\le I}\Gamma_{C,i}$ with each $\Gamma_{C,i}$ a closed line segment. Let $\mathcal{E}_h^0$ denotes all the edges of $\mathcal{T}_h$ excluding the edges on $\overline{\Gamma_D}$, and $\mathcal{P}_h^0$ denotes all the vertices of $\mathcal{T}_h$ excluding the vertices on $\overline{\Gamma_D}$. Following [30], we make assumption on the decompositions $\{\mathcal{T}_h\}_h$ as follows:

A1. There exist constants $\gamma_1 > 0$ and $\gamma_2 > 0$ such that for each h and for every $K \in \mathcal{T}_h$,
- K is star-shaped with respect to a disk of radius $\rho \ge \gamma_1 h_K$;
- the distance between any two vertices of K is no less than $\gamma_2 h_K$.

3.1. Construction of $\boldsymbol{V}_h$

Corresponding to a decomposition $\mathcal{T}_h$, we construct a finite dimensional space $\boldsymbol{V}_h \subset \boldsymbol{V}$. Similar to the virtual element method for the elasticity problem [21,31], for every element $K \in \mathcal{T}_h$ and integer $k \ge 1$, we define the local space

$$\boldsymbol{V}_h^K := \{\boldsymbol{v} \in [H^1(K)]^2 : \operatorname{div}(\mathcal{C}\boldsymbol{\varepsilon}(\boldsymbol{v})) \in [\mathbb{P}_{k-2}(K)]^2,\ \boldsymbol{v}|_{\partial K} \in C^0(\partial K),\ \boldsymbol{v}|_e \in [\mathbb{P}_k(e)]^2\ \ \forall e \subset \partial K\},$$

where $\mathbb{P}_k(K)$ denotes the space of polynomials on K of degree no more than k. Here, $\mathbb{P}_{-1}(K) = \{0\}$. Any $\boldsymbol{v} \in \boldsymbol{V}_h^K$ is determined by the following degrees of freedom (See Fig. 1.):

- the value of $\boldsymbol{v}_h$ at the vertices of K;
- the moments $\int_e \boldsymbol{q} \cdot \boldsymbol{v}_h\, ds$ for $\boldsymbol{q} \in [\mathbb{P}_{k-2}(e)]^2$ on each edge $e \subset \partial K$ for $k \ge 2$;
- the moments $\int_K \boldsymbol{q} \cdot \boldsymbol{v}_h\, d\boldsymbol{x}$ for $\boldsymbol{q} \in [\mathbb{P}_{k-2}(K)]^2$ for $k \ge 2$.

Then we define the global virtual element space as

$$\boldsymbol{V}_h := \{\boldsymbol{v} \in \boldsymbol{V} :\ \boldsymbol{v}|_K \in \boldsymbol{V}_h^K \quad \forall K \in \mathcal{T}_h\}, \tag{3.1}$$

and the global degrees of freedom for $\boldsymbol{v} \in \boldsymbol{V}_h$:

- the value of $\boldsymbol{v}_h$ at the vertices $\in \mathcal{P}_h^0$;
- the moments $\int_e \boldsymbol{q} \cdot \boldsymbol{v}_h \, ds$ for $\boldsymbol{q} \in [\mathbb{P}_{k-2}(e)]^2 \forall e \in \mathcal{E}_h^0$ for $k \geq 2$;
- the moments $\int_K \boldsymbol{q} \cdot \boldsymbol{v}_h \, d\boldsymbol{x}$ for $\boldsymbol{q} \in [\mathbb{P}_{k-2}(K)]^2 \forall K \in \mathcal{T}_h$ for $k \geq 2$.

For every smooth enough function $\boldsymbol{v}$, there exists a unique interpolation $\boldsymbol{v}_I \in V_h$ such that

$$\mathrm{dof}_i(\boldsymbol{v}_I) = \mathrm{dof}_i(\boldsymbol{v}) \quad i = 1, \ldots, N^{\mathrm{dof}},$$

where $\mathrm{dof}_i(\boldsymbol{v}_I)$ denotes the value of the ith degree of freedom of $\boldsymbol{v}_I \in V_h$. In addition, let $\boldsymbol{v}_\pi$ be a piecewise polynomial approximation of $\boldsymbol{v}$, i.e., for each element K, $(\boldsymbol{v}_\pi|_K \in [\mathbb{P}_k(K)]^2)$ is an approximation of $\boldsymbol{v}$ on K. According to the Scott–Dupont theory [32,33], we have the following approximation results.

Proposition 3.1. *If Assumption* ***A1*** *is satisfied, for any* $\boldsymbol{v} \in [H^l(\Omega)]^2$, $2 \leq l \leq k+1$, *there exist* $\boldsymbol{v}_I \in \boldsymbol{V}_h$ *and* $\boldsymbol{v}_\pi \in [\mathbb{P}_k(K)]^2$ *such that*

$$\|\boldsymbol{v} - \boldsymbol{v}_I\|_{\boldsymbol{V}} \leq c h^{l-1} |\boldsymbol{v}|_{[H^l(\Omega)]^2}, \tag{3.2}$$

$$\|\boldsymbol{v} - \boldsymbol{v}_\pi\|_{\boldsymbol{V},K} \leq c h_K^{l-1} |\boldsymbol{v}|_{[H^l(K)]^2}, \tag{3.3}$$

where $\|\boldsymbol{v}\|_{\boldsymbol{V},K}^2 := \int_K \boldsymbol{\varepsilon}(\boldsymbol{v}) : \boldsymbol{\varepsilon}(\boldsymbol{v}) dx$. *Moreover, if* $\boldsymbol{v}|_{\Gamma_{C,i}} \in H^l(\Gamma_{C,i})$, $1 \leq i \leq I$,*we have*

$$\|\boldsymbol{v} - \boldsymbol{v}_I\|_{L^2(\Gamma_C)} \leq c h^l \left(\sum_{i=1}^{I} |\boldsymbol{v}|_{l,\Gamma_{C,i}}^2 \right)^{1/2}. \tag{3.4}$$

In analysis of the virtual element method, we will use a broken norm $\|\cdot\|_{\boldsymbol{V},h}$ defined by

$$\|\boldsymbol{v}\|_{\boldsymbol{V},h}^2 = \sum_{K \in \mathcal{T}_h} \|\boldsymbol{v}\|_{\boldsymbol{V},K}^2.$$

3.2. Construction of a_h

The bilinear form $a(\cdot, \cdot)$ can be decomposed as

$$a(\boldsymbol{u}, \boldsymbol{v}) = \sum_{K \in \mathcal{T}_h} a^K(\boldsymbol{u}, \boldsymbol{v}) \quad \forall \boldsymbol{u}, \boldsymbol{v} \in \boldsymbol{V}, \tag{3.5}$$

where

$$a^K(\boldsymbol{u}, \boldsymbol{v}) = \int_K \mathcal{C} \boldsymbol{\varepsilon}(\boldsymbol{u}) : \boldsymbol{\varepsilon}(\boldsymbol{v}) \, dx.$$

Correspondingly, we will first construct suitable local bilinear form $a_h^K(\boldsymbol{u}, \boldsymbol{v})$ and then put them together as

$$a_h(\boldsymbol{u}_h, \boldsymbol{v}_h) = \sum_{K \in \mathcal{T}_h} a_h^K(\boldsymbol{u}_h, \boldsymbol{v}_h).$$

According to the general framework of virtual element method [14], the local bilinear form $a_h^K(\boldsymbol{u}, \boldsymbol{v})$ should satisfy the following properties:

- Polynomial consistency:

$$a_h^K(\boldsymbol{v}_h, \boldsymbol{q}) = a^K(\boldsymbol{v}_h, \boldsymbol{q}) \quad \forall \boldsymbol{v}_h \in \boldsymbol{V}_h^K, \ \forall \boldsymbol{q} \in [\mathbb{P}_k(K)]^2. \tag{3.6}$$

- Stability: there exist two positive constants α_* and α^*, independent of h and K, s.t.

$$\alpha_* a^K(\boldsymbol{v}_h, \boldsymbol{v}_h) \leq a_h^K(\boldsymbol{v}_h, \boldsymbol{v}_h) \leq \alpha^* a^K(\boldsymbol{v}_h, \boldsymbol{v}_h) \quad \forall \boldsymbol{v}_h \in \boldsymbol{V}_h^K. \tag{3.7}$$

Because shape functions are not available for $\boldsymbol{V}_h^K$, we cannot calculate the value of $a^K(\boldsymbol{u}, \boldsymbol{v})$ for $\boldsymbol{u}, \boldsymbol{v} \in \boldsymbol{V}_h$. Due to the computability requirement, we define a projection operator $\Pi_k^K : \boldsymbol{V}_h^K \to [\mathbb{P}_k(K)]^2$ by

$$a^K(\Pi_k^K \boldsymbol{v}_h - \boldsymbol{v}_h, \boldsymbol{q}) = 0 \quad \forall \boldsymbol{q} \in [\mathbb{P}_k(K)]^2. \tag{3.8}$$

This equation determines $\Pi_k^K \boldsymbol{v}_h$ only up to a rigid motion. In order to ensure the uniqueness, we adopt the idea in [21] to add the following conditions

$$\frac{1}{n_V^K} \sum_{i=1}^{n_V^K} \Pi_k^K \boldsymbol{v}_h(\boldsymbol{x}_i) = \frac{1}{n_V^K} \sum_{i=1}^{n_V^K} \boldsymbol{v}_h(\boldsymbol{x}_i),$$

$$\frac{1}{n_V^K}\sum_{i=1}^{n_V^K}\boldsymbol{x}_i \times \Pi_k^K \boldsymbol{v}_h(\boldsymbol{x}_i) = \frac{1}{n_V^K}\sum_{i=1}^{n_V^K}\boldsymbol{x}_i \times \boldsymbol{v}_h(\boldsymbol{x}_i),$$

where $\{\boldsymbol{x}_i\}$ are the coordinates of vertices of the element K and n_V^K denotes the number of the vertices. Then, we define the local bilinear form

$$a_h^K(\boldsymbol{u}_h, \boldsymbol{v}_h) = a^K(\Pi_k^K \boldsymbol{u}_h, \Pi_k^K \boldsymbol{v}_h) + S^K(\boldsymbol{u}_h - \Pi_k^K \boldsymbol{u}_h, \boldsymbol{v}_h - \Pi_k^K \boldsymbol{v}_h) \quad \forall\, \boldsymbol{u}_h, \boldsymbol{v}_h \in \boldsymbol{V}_h^K \tag{3.9}$$

where the stabilization term $S^K(\boldsymbol{u}_h, \boldsymbol{v}_h)$ should be chosen to satisfy

$$c_4 a^K(\boldsymbol{v}_h, \boldsymbol{v}_h) \le S^K(\boldsymbol{v}_h, \boldsymbol{v}_h) \le c_5 a^K(\boldsymbol{v}_h, \boldsymbol{v}_h) \quad \forall\, \boldsymbol{v}_h \in \boldsymbol{V}_h^K \text{ with } \Pi_k^K \boldsymbol{v}_h = \boldsymbol{0}, \tag{3.10}$$

for two positive constants c_4 and c_5. Note that (3.8)–(3.10) ensures the properties (3.6) and (3.7). In this paper, we choose

$$S^K(\boldsymbol{u}_h, \boldsymbol{v}_h) = \sum_{i=1}^{N_K^{\text{dof}}} \chi_i(\boldsymbol{u}_h)\, \chi_i(\boldsymbol{v}_h),$$

where $\chi_i(\boldsymbol{u}_h)$ denotes the ith degree of freedom for $\boldsymbol{u}_h$ and N_K^{dof} is their number.

Define

$$a_h(\boldsymbol{u}_h, \boldsymbol{v}_h) = \sum_{K\in\mathcal{T}_h} a_h^K(\boldsymbol{u}_h, \boldsymbol{v}_h) \qquad \forall \boldsymbol{u}_h, \boldsymbol{v}_h \in \boldsymbol{V}_h.$$

By the symmetry of a_h, stability (2.17) and (3.7), we have, for two positive constants C_1 and C_2,

$$a_h(\boldsymbol{v}, \boldsymbol{v}) \ge C_1 \|\boldsymbol{v}\|_{\boldsymbol{V}}^2 \quad \forall\, \boldsymbol{v} \in \boldsymbol{V}_h, \tag{3.11}$$

$$a_h(\boldsymbol{u}, \boldsymbol{v}) \le C_2 \|\boldsymbol{u}\|_{\boldsymbol{V}} \|\boldsymbol{v}\|_{\boldsymbol{V}} \quad \forall\, \boldsymbol{u}, \boldsymbol{v} \in \boldsymbol{V}_h. \tag{3.12}$$

3.3. Construction of $\boldsymbol{f}_h$

Because the term $\int_\Omega \boldsymbol{f}_1 \cdot \boldsymbol{v}\, dx$ is not computable for $\boldsymbol{v} \in \boldsymbol{V}_h$, we introduce its approximation. Let P_k^K be the L^2 projection from $\boldsymbol{V}_h^K$ to $[\mathbb{P}_k(K)]^2$. For $k = 1$, we define

$$\langle \boldsymbol{f}_{1h}, \boldsymbol{v}_h\rangle = \sum_{K\in\mathcal{T}_h}\int_K P_0^K \boldsymbol{f}_1 \cdot \boldsymbol{v}_h\, dx \quad \forall\, \boldsymbol{v}_h \in \boldsymbol{V}_h.$$

For $k \ge 2$, define

$$\langle \boldsymbol{f}_{1h}, \boldsymbol{v}_h\rangle = \sum_{K\in\mathcal{T}_h}\int_K P_{k-2}^K \boldsymbol{f}_1 \cdot \boldsymbol{v}_h\, dx \quad \forall\, \boldsymbol{v}_h \in \boldsymbol{V}_h.$$

To approximate the right-hand side term $(\boldsymbol{f}, \boldsymbol{v})$, we choose

$$\langle \boldsymbol{f}_h, \boldsymbol{v}_h\rangle = \langle \boldsymbol{f}_{1h}, \boldsymbol{v}_h\rangle + \int_{\Gamma_F} \boldsymbol{f}_2 \cdot \boldsymbol{v}_h\, ds \quad \forall\, \boldsymbol{v}_h \in \boldsymbol{V}_h.$$

Then we have the following approximation property [31]

$$\|\boldsymbol{f} - \boldsymbol{f}_h\|_{\boldsymbol{V}_h'} = \sup_{\boldsymbol{v}_h\in\boldsymbol{V}_h} \frac{(\boldsymbol{f}, \boldsymbol{v}_h) - \langle \boldsymbol{f}_h, \boldsymbol{v}_h\rangle}{\|\boldsymbol{v}_h\|_{\boldsymbol{V}}} \le c\, h^k |\boldsymbol{f}|_{k-1}. \tag{3.13}$$

Also,

$$(\boldsymbol{f}, \boldsymbol{v}_h) - \langle \boldsymbol{f}_h, \boldsymbol{v}_h\rangle \le \|\boldsymbol{f} - \boldsymbol{f}_h\|_{\boldsymbol{V}_h'} \|\boldsymbol{v}_h\|_{\boldsymbol{V}} \quad \forall \boldsymbol{v}_h \in \boldsymbol{V}_h. \tag{3.14}$$

Furthermore, by the property of the L^2 projection operator P_k^K, we have

$$\langle \boldsymbol{f}_h, \boldsymbol{v}_h\rangle \le c\|\boldsymbol{v}_h\|_{\boldsymbol{V}} \quad \forall \boldsymbol{v}_h \in \boldsymbol{V}_h \tag{3.15}$$

where the constant c depends only on $\boldsymbol{f}_1$ and $\boldsymbol{f}_2$.

3.4. The discrete problem

We introduce the discrete scheme for solving the Problem (P).

Problem ($\mathbf{P_h}$). Find a displacement field $\boldsymbol{u}_h \in \boldsymbol{V}_h$, such that

$$a_h(\boldsymbol{u}_h, \boldsymbol{v}_h - \boldsymbol{u}_h) + j(\boldsymbol{u}_h, \boldsymbol{v}_h) - j(\boldsymbol{u}_h, \boldsymbol{u}_h) \ge \langle \boldsymbol{f}_h, \boldsymbol{v}_h - \boldsymbol{u}_h\rangle \quad \forall\, \boldsymbol{v}_h \in \boldsymbol{V}_h. \tag{3.16}$$

Let us prove the existence and uniqueness of the numerical solution of the discrete problem (3.16).

Theorem 3.2. *Assume $\boldsymbol{f}_1 \in [L^2(\Omega)]^2$, $\boldsymbol{f}_2 \in [L^2(\Gamma_F)]^2$, the gap function $g_a \in L^2(\Gamma_C)$, and p_e $(e = \nu, \tau)$ satisfies the conditions (2.10). Moreover, we assume the smallness condition $C_1 > C_0^2(L_\nu + L_\tau)$. Then,* Problem $(\mathrm{P_h})$ *has a unique solution.*

Proof. First, we define the operator $A : \boldsymbol{V}_h \to \boldsymbol{V}_h$ by

$$(A\boldsymbol{u}_h, \boldsymbol{v}_h)_{\boldsymbol{V}_h} = a_h(\boldsymbol{u}_h, \boldsymbol{v}_h). \tag{3.17}$$

By the continuity (3.12) of a_h, we see that A is a Lipschitz continuous operator on $\boldsymbol{V}_h$. Furthermore, from (3.11), the coerciveness of a_h, we get

$$(A\boldsymbol{u}_h - A\boldsymbol{v}_h, \boldsymbol{u}_h - \boldsymbol{v}_h)_{\boldsymbol{V}_h} = a_h(\boldsymbol{u}_h - \boldsymbol{v}_h, \boldsymbol{u}_h - \boldsymbol{v}_h) \ge C_1 \|\boldsymbol{u}_h - \boldsymbol{v}_h\|_{\boldsymbol{V}}^2.$$

So A is strongly monotone. From the definition of j in (2.15) and the assumption (2.10), we see that for all $\boldsymbol{v} \in \boldsymbol{V}_h$, the functional $j(\boldsymbol{v}, \cdot) : \boldsymbol{V}_h \to \mathbb{R}$ is continuous. For any $\boldsymbol{u}_1, \boldsymbol{u}_2, \boldsymbol{v}_1, \boldsymbol{v}_2 \in \boldsymbol{V}_h$, using (2.16) and (2.19), we obtain

$$\begin{aligned} j(\boldsymbol{u}_1, \boldsymbol{v}_2) - j(\boldsymbol{u}_1, \boldsymbol{v}_1) + j(\boldsymbol{u}_2, \boldsymbol{v}_1) - j(\boldsymbol{u}_2, \boldsymbol{v}_2) &\le (L_\nu + L_\tau)\|\boldsymbol{u}_1 - \boldsymbol{u}_2\|_{L^2(\Gamma_C)} \|\boldsymbol{v}_1 - \boldsymbol{v}_2\|_{L^2(\Gamma_C)} \\ &\le C_0^2(L_\nu + L_\tau)\|\boldsymbol{u}_1 - \boldsymbol{u}_2\|_{\boldsymbol{V}} \|\boldsymbol{v}_1 - \boldsymbol{v}_2\|_{\boldsymbol{V}}. \end{aligned}$$

From (3.15), we see that $\boldsymbol{f}_h \in \boldsymbol{V}_h'$. Thus, applying [2, Theorem 2.19], under the stated assumptions, we conclude that Problem $(\mathrm{P_h})$ has a unique solution. ■

4. Error estimates

In this section, we derive error estimates for the VEM solutions of Problem (P). First, we provide a uniform boundedness result on the numerical solution $\boldsymbol{u}_h$.

Lemma 4.1. *Under the assumptions stated in Theorem 3.2, the numerical solution $\boldsymbol{u}_h \in \boldsymbol{V}_h$ of* Problem $(\mathrm{P_h})$ *is uniformly bounded independent of h.*

Proof. Let $\boldsymbol{v}_h = \boldsymbol{0}$ in (3.16),

$$a_h(\boldsymbol{u}_h, -\boldsymbol{u}_h) + j(\boldsymbol{u}_h, \boldsymbol{0}) - j(\boldsymbol{u}_h, \boldsymbol{u}_h) \ge \langle \boldsymbol{f}_h, -\boldsymbol{u}_h \rangle,$$

so

$$a_h(\boldsymbol{u}_h, \boldsymbol{u}_h) \le j(\boldsymbol{u}_h, \boldsymbol{0}) - j(\boldsymbol{u}_h, \boldsymbol{u}_h) + \langle \boldsymbol{f}_h, \boldsymbol{u}_h \rangle. \tag{4.1}$$

By the definition of $j(\boldsymbol{u}, \boldsymbol{v})$, it is easy to see that $j(\boldsymbol{0}, \boldsymbol{v}) = 0$ for any $\boldsymbol{v} \in \boldsymbol{V}$. And from (2.16) and trace inequality (2.19), we get

$$j(\boldsymbol{u}_h, \boldsymbol{0}) - j(\boldsymbol{u}_h, \boldsymbol{u}_h) \le (L_\nu + L_\tau)\|\boldsymbol{u}_h\|_{L^2(\Gamma_C)}^2 \le C_0^2(L_\nu + L_\tau)\|\boldsymbol{u}_h\|_{\boldsymbol{V}}^2. \tag{4.2}$$

Use (3.15), (3.11) and (4.2) in (4.1) to obtain

$$(C_1 - C_0^2(L_\nu + L_\tau))\|\boldsymbol{u}_h\|_{\boldsymbol{V}}^2 \le c\|\boldsymbol{u}_h\|_{\boldsymbol{V}}.$$

Since $C_1 > C_0^2(L_\nu + L_\tau)$,

$$\|\boldsymbol{u}_h\|_{\boldsymbol{V}} \le \frac{c}{C_1 - C_0^2(L_\nu + L_\tau)},$$

which completes the proof. ■

Now we are ready to give an error estimate for the VEM solution of Problem (P).

Theorem 4.2. *Let $\boldsymbol{u}$ and $\boldsymbol{u}_h$ be the solutions of* Problem (P) *and* Problem $(\mathrm{P_h})$*, respectively. Then*

$$\|\boldsymbol{u} - \boldsymbol{u}_h\|_{\boldsymbol{V}} \le c\left(\|\boldsymbol{u} - \boldsymbol{u}_\pi\|_{\boldsymbol{V},h} + \|\boldsymbol{u} - \boldsymbol{u}_I\|_{\boldsymbol{V},h} + \|\boldsymbol{f} - \boldsymbol{f}_h\|_{\boldsymbol{V}_h'} + \|\boldsymbol{u} - \boldsymbol{u}_I\|_{L^2(\Gamma_C)}^{1/2}\right), \tag{4.3}$$

where $\boldsymbol{u}_I$ and $\boldsymbol{u}_\pi$ are approximations of $\boldsymbol{u}$ defined in Section 3.1.

Proof. First, we split the error $\boldsymbol{e} = \boldsymbol{u} - \boldsymbol{u}_h$ into two parts

$$\boldsymbol{e} = \boldsymbol{e}_I + \boldsymbol{e}_h,$$

where

$$\boldsymbol{e}_I = \boldsymbol{u} - \boldsymbol{u}_I, \quad \boldsymbol{e}_h = \boldsymbol{u}_I - \boldsymbol{u}_h,$$

and $\boldsymbol{u}_I \in \boldsymbol{V}_h$ is the interpolation of $\boldsymbol{u}$. Setting $\boldsymbol{v}_h = \boldsymbol{e}_h \in \boldsymbol{V}_h$ in (3.11), we get

$$C_1 \|\boldsymbol{e}_h\|_{\boldsymbol{V}}^2 \le a_h(\boldsymbol{e}_h, \boldsymbol{e}_h) = a_h(\boldsymbol{u}_I, \boldsymbol{e}_h) - a_h(\boldsymbol{u}_h, \boldsymbol{e}_h). \tag{4.4}$$

By (3.6), we have

$$\begin{aligned} a_h(\boldsymbol{u}_I, \boldsymbol{e}_h) &= \sum_{K\in\mathcal{T}_h} (a_h^K(\boldsymbol{u}_I - \boldsymbol{u}_\pi, \boldsymbol{e}_h) + a_h^K(\boldsymbol{u}_\pi, \boldsymbol{e}_h)) \\ &= \sum_{K\in\mathcal{T}_h} (a_h^K(\boldsymbol{u}_I - \boldsymbol{u}_\pi, \boldsymbol{e}_h) + a^K(\boldsymbol{u}_\pi, \boldsymbol{e}_h)) \\ &= \sum_{K\in\mathcal{T}_h} (a_h^K(\boldsymbol{u}_I - \boldsymbol{u}_\pi, \boldsymbol{e}_h) + a^K(\boldsymbol{u}_\pi - \boldsymbol{u}, \boldsymbol{e}_h)) + a(\boldsymbol{u}, \boldsymbol{e}_h). \end{aligned} \tag{4.5}$$

From the discrete virtual element scheme (3.16),

$$-a_h(\boldsymbol{u}_h, \boldsymbol{u}_I - \boldsymbol{u}_h) \le -\langle \boldsymbol{f}_h, \boldsymbol{u}_I - \boldsymbol{u}_h\rangle - j(\boldsymbol{u}_h, \boldsymbol{u}_h) + j(\boldsymbol{u}_h, \boldsymbol{u}_I). \tag{4.6}$$

Combining (4.4)–(4.6), we have

$$C_1 \|\boldsymbol{e}_h\|_{\boldsymbol{V}}^2 \le R_1 + R_2 + R_3, \tag{4.7}$$

where

$$\begin{aligned} R_1 &= \sum_{K\in\mathcal{T}_h} (a_h^K(\boldsymbol{u}_I - \boldsymbol{u}_\pi, \boldsymbol{e}_h) + a^K(\boldsymbol{u}_\pi - \boldsymbol{u}, \boldsymbol{e}_h)), \\ R_2 &= (\boldsymbol{f}, \boldsymbol{e}_h) - \langle \boldsymbol{f}_h, \boldsymbol{e}_h\rangle, \\ R_3 &= a(\boldsymbol{u}, \boldsymbol{e}_h) - (\boldsymbol{f}, \boldsymbol{e}_h) - j(\boldsymbol{u}_h, \boldsymbol{u}_h) + j(\boldsymbol{u}_h, \boldsymbol{u}_I). \end{aligned}$$

Let us bound each of the terms on the right side of (4.7). From the continuity of each a^K and Cauchy–Schwarz inequality,

$$R_1 \le c \left(\left(\sum_{K\in\mathcal{T}_h} \|\boldsymbol{u}_I - \boldsymbol{u}_\pi\|_{\boldsymbol{V},K}^2 \right)^{1/2} + \left(\sum_{K\in\mathcal{T}_h} \|\boldsymbol{u} - \boldsymbol{u}_\pi\|_{\boldsymbol{V},K}^2 \right)^{1/2} \right) \|\boldsymbol{e}_h\|_{\boldsymbol{V}}. \tag{4.8}$$

From (3.15),

$$R_2 \le c \|\boldsymbol{f} - \boldsymbol{f}_h\|_{\boldsymbol{V}_h'} \|\boldsymbol{e}_h\|_{\boldsymbol{V}}. \tag{4.9}$$

Taking $\boldsymbol{v} = \boldsymbol{u}_h$ or $\boldsymbol{v} = 2\boldsymbol{u} - \boldsymbol{u}_I$ in (2.13), we get

$$a(\boldsymbol{u}, \boldsymbol{u} - \boldsymbol{u}_h) \le (\boldsymbol{f}, \boldsymbol{u} - \boldsymbol{u}_h) + j(\boldsymbol{u}, \boldsymbol{u}_h) - j(\boldsymbol{u}, \boldsymbol{u}), \tag{4.10}$$

and

$$a(\boldsymbol{u}, \boldsymbol{u}_I - \boldsymbol{u}) \le (\boldsymbol{f}, \boldsymbol{u}_I - \boldsymbol{u}) - j(\boldsymbol{u}, \boldsymbol{u}) + j(\boldsymbol{u}, 2\boldsymbol{u} - \boldsymbol{u}_I). \tag{4.11}$$

Therefore,

$$\begin{aligned} R_3 &= a(\boldsymbol{u}, \boldsymbol{u}_I - \boldsymbol{u}) + a(\boldsymbol{u}, \boldsymbol{u} - \boldsymbol{u}_h) - (\boldsymbol{f}, \boldsymbol{e}_h) - j(\boldsymbol{u}_h, \boldsymbol{u}_h) + j(\boldsymbol{u}_h, \boldsymbol{u}_I) \\ &\le \big(j(\boldsymbol{u}, 2\boldsymbol{u} - \boldsymbol{u}_I) - j(\boldsymbol{u}, \boldsymbol{u})\big) + \big(j(\boldsymbol{u}_h, \boldsymbol{u}_I) - j(\boldsymbol{u}_h, \boldsymbol{u})\big) \\ &\quad + \big(j(\boldsymbol{u}, \boldsymbol{u}_h) - j(\boldsymbol{u}, \boldsymbol{u}) + j(\boldsymbol{u}_h, \boldsymbol{u}) - j(\boldsymbol{u}_h, \boldsymbol{u}_h)\big). \end{aligned} \tag{4.12}$$

From (2.16),

$$j(\boldsymbol{u}, \boldsymbol{u}_h) - j(\boldsymbol{u}, \boldsymbol{u}) + j(\boldsymbol{u}_h, \boldsymbol{u}) - j(\boldsymbol{u}_h, \boldsymbol{u}_h) \le (L_\nu + L_\tau) \|\boldsymbol{u} - \boldsymbol{u}_h\|_{L^2(\Gamma_C)}^2. \tag{4.13}$$

By the definition of $j(\boldsymbol{u}, \boldsymbol{v})$, it is easy to see that $j(\boldsymbol{0}, \boldsymbol{v}) = 0$ for any $\boldsymbol{v} \in \boldsymbol{V}$. So

$$\begin{aligned} j(\boldsymbol{u}, 2\boldsymbol{u} - \boldsymbol{u}_I) - j(\boldsymbol{u}, \boldsymbol{u}) &= j(\boldsymbol{u}, 2\boldsymbol{u} - \boldsymbol{u}_I) - j(\boldsymbol{u}, \boldsymbol{u}) + j(\boldsymbol{0}, 2\boldsymbol{u} - \boldsymbol{u}_I) - j(\boldsymbol{0}, \boldsymbol{u}) \\ &\le (L_\nu + L_\tau) \|\boldsymbol{u}\|_{L^2(\Gamma_C)} \|\boldsymbol{u} - \boldsymbol{u}_I\|_{L^2(\Gamma_C)}. \end{aligned} \tag{4.14}$$

Similarly, we get

$$j(\boldsymbol{u}_h, \boldsymbol{u}_I) - j(\boldsymbol{u}_h, \boldsymbol{u}) \le (L_\nu + L_\tau) \|\boldsymbol{u}_h\|_{L^2(\Gamma_C)} \|\boldsymbol{u} - \boldsymbol{u}_I\|_{L^2(\Gamma_C)}. \tag{4.15}$$

Using (4.13)–(4.15) in (4.12) and Lemma 4.1, as well as the trace inequality (2.19), we obtain

$$R_3 \le C_0^2 (L_\nu + L_\tau) \|\boldsymbol{u} - \boldsymbol{u}_h\|_{\boldsymbol{V}}^2 + c(L_\nu + L_\tau) \|\boldsymbol{u} - \boldsymbol{u}_I\|_{L^2(\Gamma_C)}. \tag{4.16}$$

Combine (4.8), (4.9), (4.16) and triangle inequality with (4.7),

$$C_1\|\boldsymbol{e}_h\|_{\boldsymbol{V}}^2 \le c\left(\|\boldsymbol{u}-\boldsymbol{u}_\pi\|_{\boldsymbol{V},h} + \|\boldsymbol{u}-\boldsymbol{u}_I\|_{\boldsymbol{V}} + \|\boldsymbol{f}-\boldsymbol{f}_h\|_{\boldsymbol{V}_h'}\right)\|\boldsymbol{e}_h\|_{\boldsymbol{V}} + C_0^2(L_\nu+L_\tau)\|\boldsymbol{u}-\boldsymbol{u}_h\|_{\boldsymbol{V}}^2 + c(L_\nu+L_\tau)\|\boldsymbol{u}-\boldsymbol{u}_I\|_{L^2(\Gamma_C)}. \tag{4.17}$$

Applying the fact that

$$a, b, x > 0 \text{ and } x^2 \le ax + b \quad \Longrightarrow \quad x \le a + b^{1/2},$$

we arrive at

$$\|\boldsymbol{e}_h\|_{\boldsymbol{V}} \le c\left(\|\boldsymbol{u}-\boldsymbol{u}_\pi\|_{\boldsymbol{V},h} + \|\boldsymbol{u}-\boldsymbol{u}_I\|_{\boldsymbol{V}} + \|\boldsymbol{f}-\boldsymbol{f}_h\|_{\boldsymbol{V}_h'}\right) + \sqrt{\frac{C_0^2(L_\nu+L_\tau)}{C_1}}\|\boldsymbol{u}-\boldsymbol{u}_h\|_{\boldsymbol{V}} + c^{1/2}(L_\nu+L_\tau)^{1/2}\|\boldsymbol{u}-\boldsymbol{u}_I\|_{L^2(\Gamma_C)}^{1/2}.$$

By the triangle inequality

$$\|\boldsymbol{u}-\boldsymbol{u}_h\|_{\boldsymbol{V}} \le \|\boldsymbol{u}-\boldsymbol{u}_I\|_{\boldsymbol{V}} + \|\boldsymbol{e}_h\|_{\boldsymbol{V}}, \tag{4.18}$$

and noting that $C_1 > C_0^2(L_\nu + L_\tau)$, we obtain the inequality (4.3). ■

Generally, variational inequalities have low regularities, so it makes sense to only use lowest-order numerical schemes. For the lowest-order VEM, i.e., $k = 1$, if $\boldsymbol{u} \in (H^2(\Omega))^2$ and $\boldsymbol{u}|_{\Gamma_{C,i}} \in H^2(\Gamma_{C,i})$, $1 \le i \le I$, from the approximation properties (3.2)–(3.4), we have

$$\|\boldsymbol{u}-\boldsymbol{u}_\pi\|_{\boldsymbol{V},h} \le ch|\boldsymbol{u}|_{2,\Omega},$$

$$\|\boldsymbol{u}-\boldsymbol{u}_I\|_{\boldsymbol{V}} \le ch|\boldsymbol{u}|_{2,\Omega},$$

and

$$\|\boldsymbol{u}-\boldsymbol{u}_I\|_{L^2(\Gamma_C)} \le ch^2\left(\sum_{i=1}^{I}|\boldsymbol{u}|_{2,\Gamma_{C,i}}^2\right)^{1/2}.$$

Therefore, we obtain

$$\|\boldsymbol{u}-\boldsymbol{u}_h\|_{\boldsymbol{V}} \le ch,$$

which is an optimal order error estimate.

For high order VEM, due to the inequality form of the problem, it is not possible to have an optimal order error estimate, even if the solution is smooth. For example, when $k = 2$, even under higher solution regularities $\boldsymbol{u} \in (H^3(\Omega))^2$ and $\boldsymbol{u}|_{\Gamma_{C,i}} \in H^3(\Gamma_{C,i})$, $1 \le i \le I$, we can only get suboptimal convergence order

$$\|\boldsymbol{u}-\boldsymbol{u}_h\|_{\boldsymbol{V}} \le ch^{3/2}$$

due to the contact boundary error approximation result (3.4) for $l = 3$. One way to improve convergence order is to refine the elements along contact boundary Γ_C to reduce the error $\|\boldsymbol{u}-\boldsymbol{u}_I\|_{L^2(\Gamma_C)}$. Such a mesh refinement can be easily obtained for the virtual element method because it treats the hanging nodes as vertices of the new element. It is an advantage of VEM to solve contact problems.

5. Numerical simulations

In this section, we report some numerical simulation results.

In the numerical experiment, we consider functions p_ν, p_τ in the form

$$p_\nu(t) = k_\nu(t)_+^{m_\nu}, \quad p_\tau(t) = k_\tau(t)_+^{m_\tau}, \tag{5.1}$$

where $k_\nu, m_\nu, k_\tau, m_\tau \ge 0$, and $(t)_+ = \max\{t, 0\}$. We can verify that the function p_ν and p_τ satisfy the condition (2.10). For simplicity, we consider a reduced normal compliance law, i.e. $m_\tau = 0$ in (5.1); then the functional $j(\boldsymbol{u}, \boldsymbol{v})$ can be written as

$$j(\boldsymbol{u}, \boldsymbol{v}) = j_\nu(\boldsymbol{u}, \boldsymbol{v}) + j_\tau(\boldsymbol{v}),$$

where

$$j_\nu(\boldsymbol{u}, \boldsymbol{v}) = \int_{\Gamma_C} k_\nu(u_\nu - g_a)_+^{m_\nu} v_\nu ds,$$

Table 1
Errors and numerical convergence orders of the lowest order VEM.

h	2^{-2}	2^{-3}	2^{-4}	2^{-5}	2^{-6}
Error	1.9114e−1	1.0309e−1	5.4352e−2	2.80070e−2	1.3828e−2
Convergence order	–	0.89067	0.92354	0.95656	1.0182

$$j_\tau(\boldsymbol{v}) = \int_{\Gamma_C} k_\tau |\boldsymbol{v}_\tau| ds.$$

In order to implement the virtual element method (3.16), we use the Uzawa iteration by introducing a Lagrange multiplier $\boldsymbol{\lambda}_h$ [34]. Then the discrete problem (3.16) is equivalent to the system

$$a_h(\boldsymbol{u}_h, \boldsymbol{v}_h) + j_\nu(\boldsymbol{u}_h, \boldsymbol{v}_h) + \int_{\Gamma_C} k_\tau \boldsymbol{\lambda}_{h\tau} \cdot \boldsymbol{v}_{h\tau} ds = \langle \boldsymbol{f}_h, \boldsymbol{v}_h \rangle \quad \forall \boldsymbol{v}_h \in V_h, \tag{5.2}$$

$$|\boldsymbol{\lambda}_{h\tau}| \le 1, \quad \boldsymbol{\lambda}_{h\tau} \cdot \boldsymbol{u}_{h\tau} = |\boldsymbol{u}_{h\tau}| \quad \text{a.e. on } \Gamma_C. \tag{5.3}$$

Since the spatial domain of the problem is two-dimensional, $\boldsymbol{\lambda}_{h\tau}$ and $\boldsymbol{v}_{h\tau}$ can be equivalently viewed as scalars, e.g., we use $v_{h\tau} \equiv \boldsymbol{v}_{h\tau} \cdot \boldsymbol{\tau}$ to replace $\boldsymbol{v}_{h\tau}$. Then, the Uzawa iteration algorithm is as follows.

Step 1 Choose $\lambda_{h\tau}^{(0)} = 0$ and $\boldsymbol{u}_h^{(0)} = \boldsymbol{0}$.

Step 2 For $n = 1, 2, \ldots$, find $\boldsymbol{u}_h^{(n)} \in V_h$ such that

$$a_h(\boldsymbol{u}_h^{(n)}, \boldsymbol{v}_h) = \langle \boldsymbol{f}_h, \boldsymbol{v}_h \rangle - j_\nu(\boldsymbol{u}_h^{(n-1)}, \boldsymbol{v}_h) - \int_{\Gamma_C} k_\tau \lambda_{h\tau}^{(n-1)} v_{h\tau}\, ds \quad \forall \boldsymbol{v}_h \in V_h. \tag{5.4}$$

Then, update the Lagrangian multiplier

$$\lambda_{h\tau}^{(n)} = P\left(\lambda_{h\tau}^{(n-1)} + \rho k_\tau u_{h\tau}^{(n)}\right), \tag{5.5}$$

where ρ is a positive constant and P is a projection operator defined by

$$P(\mu) = \sup\big(-1, \inf(1, \mu)\big) \quad \forall \mu \in L^\infty(\Gamma_C). \tag{5.6}$$

Step 3 If $\|\boldsymbol{u}^{(n)} - \boldsymbol{u}^{(n-1)}\| < \epsilon_1$ or $|\lambda_{h\tau}^{(n)} - \lambda_{h\tau}^{(n-1)}| < \epsilon_2$, for two given error tolerances $\epsilon_1 > 0$ and $\epsilon_2 > 0$, stop; otherwise, go to **Step2**.

For numerical simulations, let $\Omega = (0, 1) \times (0, 1) \subset \mathbb{R}^2$ with $\Gamma_D = \{1\} \times (0, 1)$, $\Gamma_F = (\{0\} \times (0, 1)) \cup ((0, 1) \times \{1\})$, and $\Gamma_C = (0, 1) \times \{0\}$. The domain Ω represents the cross-section of a three-dimensional deformable body. The physical setting is shown in Fig. 2. The elasticity tensor $\mathcal{C}$ is given by

$$(\mathcal{C}\boldsymbol{\varepsilon})_{ij} = \frac{E\kappa}{1-\kappa^2}(\varepsilon_{11} + \varepsilon_{22})\delta_{ij} + \frac{E}{1+\kappa}\varepsilon_{ij}, \quad 1 \le i, j \le 2,$$

where E is the Young's modulus, κ is the Poisson ratio of the material and δ_{ij} denotes the Kronecker symbol. We use the following data (the unit daN/mm^2 stands for "decaNewtons per square millimeter"):

$$E = 2000\,\text{daN/mm}^2, \quad \kappa = 0.4, \quad \boldsymbol{f}_1 = (0, 0)\,\text{daN/mm}^2$$
$$\boldsymbol{f}_2(x_1, x_2) = \begin{cases} (0, 0)\,\text{daN/mm} & \text{on } [0, 1] \times \{1\}, \\ (200(5 - x_2), -200)\,\text{daN/mm} & \text{on } \{0\} \times [0, 1], \end{cases}$$
$$k_\tau = 450, \quad k_\nu = 10, \quad m_\nu = 1, \quad g_a = 0.1\,\text{mm}.$$

First, we solve the problem on square meshes for computing the numerical errors. We use a uniform partition of the interval [0, 1] and denote by $1/h$ the number of sub-intervals of [0, 1]. In Table 1, we report the H^1 error of the numerical solutions and the corresponding convergence orders. Since the true solution $\boldsymbol{u}$ is not available, we use the numerical solution on a fine mesh as the "reference" solution $\boldsymbol{u}_{ref}$. Specifically, we use the numerical solution with $h = 2^{-8}$ as the "reference" solution. Because the virtual element solution $\boldsymbol{u}_h$ is not computable, instead, we compute the relative error $\left\|\Pi_1(\boldsymbol{u}_h - \boldsymbol{u}_{ref})\right\|_{H^1} / \left\|\Pi_1\boldsymbol{u}_{ref}\right\|_{H^1}$, where the restriction of the projection Π_1 on K is defined by (3.8). We observe that the numerical convergence orders are close to one, which matches well the theoretical prediction.

Furthermore, we solve the same contact problem on two other meshes. In Fig. 4, we show the numerical solution $\boldsymbol{u} = (u_1, u_2)^T$ on unstructured triangular mesh with 1024 triangles. The numerical solution on a polygonal mesh with 1024 polygons is shown in Fig. 5. Comparing with the numerical solution on square mesh in Fig. 3, the displacements u_1 and u_2 on these meshes are almost the same, which shows that the virtual element method works well on general meshes.

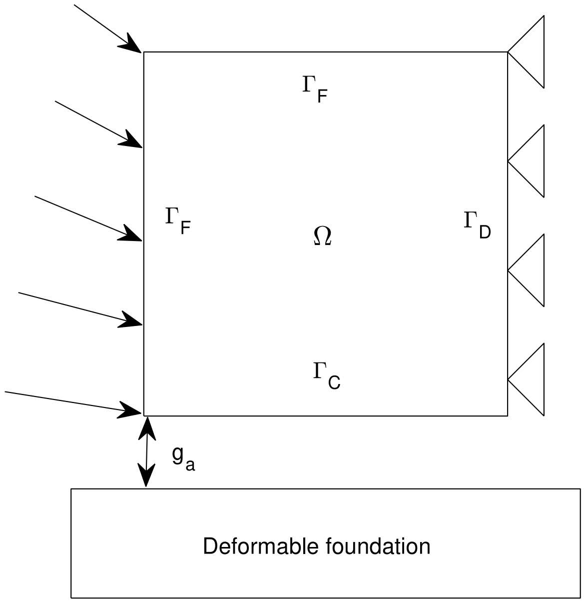

Fig. 2. Physical configuration.

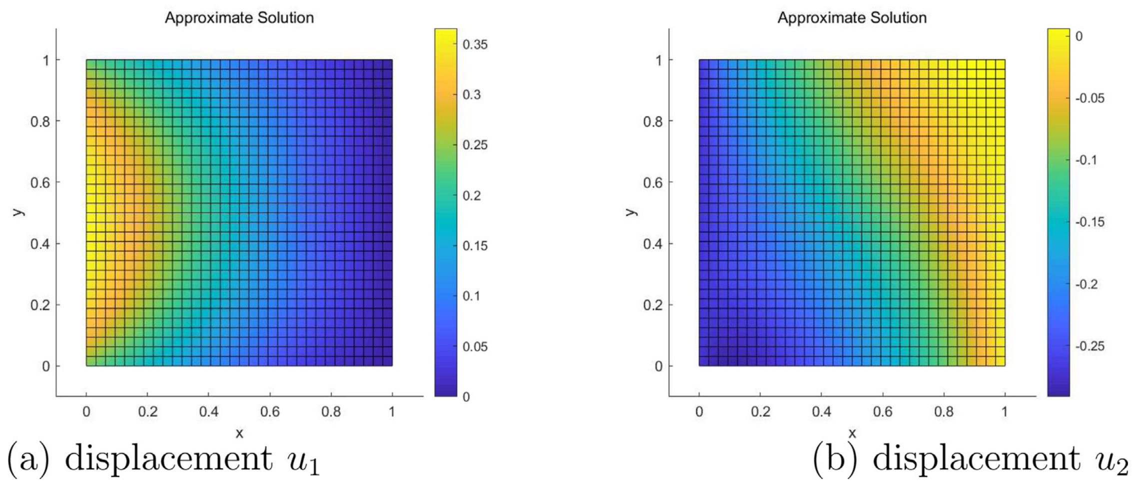

Fig. 3. Numerical solution on square mesh (1024 squares)

Fig. 6 shows the deformed mesh with a magnification of the displacement with $h = 1/16$. We observe that the penetration occurs at the contact interface, the value of u_ν exceed $g = 0.1$ in certain interval. The gray color represents the value of the elastic shear energy density $|\mathrm{dev}\boldsymbol{\sigma}|^2/(4\mu)$ [35], where

$$|\mathrm{dev}\boldsymbol{\sigma}|^2 = \left(\frac{\mu^2}{6(\mu+\lambda)^2} + \frac{1}{2}\right)(\sigma_{11}+\sigma_{22})^2 + 2(\sigma_{12}^2 - \sigma_{11}\sigma_{22}).$$

CRediT authorship contribution statement

Bangmin Wu: Methodology, Software, Formal analysis, Visualization, Data curation, Writing – original draft. **Fei Wang:** Conceptualization, Writing – original draft, Writing – review & editing, Project administration, Funding acquisition. **Weimin Han:** Supervision, Writing – review & editing.

Declaration of competing interest

The authors declare that they have no known competing financial interests or personal relationships that could have appeared to influence the work reported in this paper.

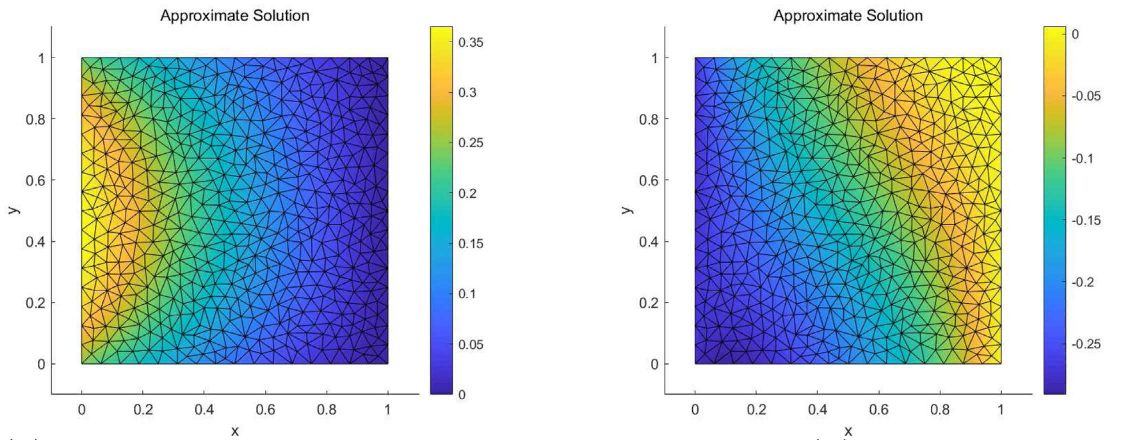

(a) displacement u_1 (b) displacement u_2

Fig. 4. Numerical solution on unstructured triangle mesh (1024 triangles)

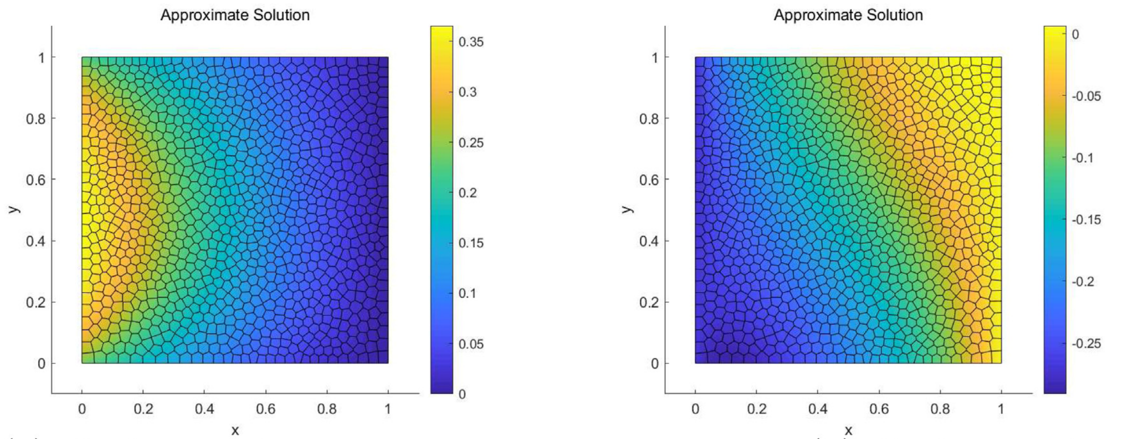

(a) displacement u_1 (b) displacement u_2

Fig. 5. Numerical solution on polygonal mesh (1024 polygons)

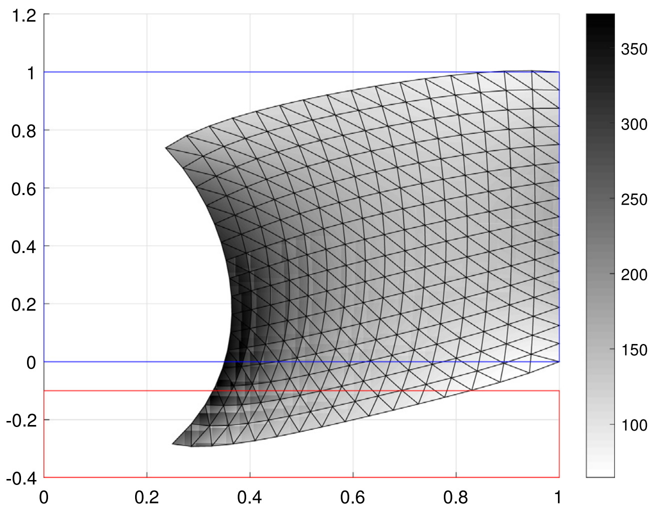

Fig. 6. Deformed configuration with $h = 1/16$.

References

[1] Han W, Sofonea M. Analysis and numerical approximation of an elastic frictional contact problem with normal compliance. Appl Math 1999;25:415–35.
[2] Sofonea M, Matei A. Mathematical models in contact mechanics. Cambridge University Press; 2012.
[3] Khan A, Migorski S, Sama M. Inverse problems for multi-valued quasi variational inequalities and noncoercive variational inequalities with noisy data. Optimization 2019;68:1897–931.
[4] Migórski S, Khan A, Zeng S. Inverse problems for nonlinear quasi-variational inequalities with an application to implicit obstacle problems of p-Laplacian type. Inverse Problems 2019;35:035004.
[5] Han W. On the numerical approximation of a frictional contact problem with normal compliance. Numer Funct Anal Optim 1996;17:307–22.
[6] Lee CY, Oden JT. A priori error estimation of *hp*-finite element approximations of frictional contact problems with normal compliance. Int J Eng Sci 1993;31:927–52.
[7] Han W, Shillor M, Sofonea M. Variational and numerical analysis of a quasistatic viscoelastic problem with normal compliance, friction and damage. J Comput Appl Math 2001;137:377–98.
[8] Amassad A, Fabre C, Sofonea M. A quasistatic viscoplastic contact problem with normal compliance and friction. IMA J Appl Math 2004;69:463–82.
[9] Xiao W, Wang F, Han W. Discontinuous Galerkin methods for solving a frictional contact problem with normal compliance. Numer Funct Anal Optim 2018;39:1248–64.
[10] Wang F, Shah S, Xiao W. A priori error estimates of discontinuous Galerkin methods for a quasi-variational inequality. BIT 2021;61:1005–22.
[11] Chouly F, Hild P. A nitsche-based method for unilateral contact problems: numerical analysis. SIAM J Numer Anal 2013;51:1295–307.
[12] Chouly F, Mlika R, Renard Y. An unbiased Nitsche's approximation of the frictional contact between two elastic structures. Numer Math 2018;139:593–631.
[13] Cascavita KL, Chouly F, Ern A. Hybrid high-order discretizations combined with Nitsche's method for Dirichlet and signorini boundary conditions. IMA J Numer Anal 2020;40:2189–226.
[14] Beirão da Veiga L, Brezzi F, Cangiani A, Manzini G, Marini LD, Russo A. Basic principles of virtual element methods. Math Models Methods Appl Sci 2013;23:199–214.
[15] Gain AL, Talischi C, Paulino GH. On the virtual element method for three-dimensional elasticity problems on arbitrary polyhedral meshes. Comput Methods Appl Mech Engrg 2014;282:132–60.
[16] Antonietti PF, Beirão da Veiga L, Scacchi S, Verani M. A C^1 virtual element method for the Cahn-Hilliard equation with polygonal meshes. SIAM J Numer Anal 2016;54:34–56.
[17] Benedetto MF, Berrone S, Borio A, Pieraccini S, Scialo S. Order preserving SUPG stabilization for the virtual element formulation of advection-diffusion problems. Comput Methods Appl Mech Engrg 2016;311:18–40.
[18] Perugia I, Pietra P, Russo A. A plane wave virtual element method for the Helmholtz problem. ESAIM: M2AN 2016;50:783–808.
[19] Zhao J, Chen S, Zhang B. The nonconforming virtual element method for plate bending problems. Math Models Methods Appl Sci 2016;26:1671–87.
[20] Beirão da Veiga L, Lovadina C, Vacca G. Virtual elements for the Navier–Stokes problem on polygonal meshes. SIAM J Numer Anal 2018;56:1210–42.
[21] Wriggers P, Rust WT, Reddy BD. A virtual element method for contact. Comput Mech 2016;58:1039–50.
[22] Wang F, Wei H. Virtual element method for simplified friction problem. Appl Math Lett 2018;85:125–31.
[23] Wang F, Wei H. Virtual element methods for obstacle problem. IMA J Numer Anal 2020;40:708–28.
[24] Feng F, Han W, Huang J. Virtual element methods for elliptic variational inequalities of the second kind. J Sci Comput 2019;80:60–80.
[25] Feng F, Han W, Huang J. Virtual element method for an elliptic hemivariational inequality with applications to contact mechanics. J Sci Comput 2019;81:2388–412.
[26] Wang F, Wu B, Han W. The virtual element method for general elliptic hemivariational inequalities. J Comput Appl Math 2021;389:113330.
[27] Wang F, Zhao J. Conforming and nonconforming virtual element methods for a Kirchhoff plate contact problem. IMA J Numer Anal 2021;41:1496–521.
[28] Ling M, Wang F, Han W. The nonconforming virtual element method for a stationary stokes hemivariational inequality with slip boundary condition. J Sci Comput 2020;85. article number 56.
[29] Nečas J, Hlaváček I. Mathematical theory of elastic and elastico-plastic bodies: an introduction. Amsterdam, Oxford, New York: Elsevier Scientific Publishing Company; 1981.
[30] Beirão da Veiga L, Lovadina C, Russo A. Stability analysis for the virtual element method. Math Models Methods Appl Sci 2017;27:2557–94.
[31] Beirão da Veiga L, Brezzi F, Marini LD. Virtual elements for linear elasticity problems. SIAM J Numer Anal 2013;51:794–812.
[32] Ciarlet PG. The finite element method for elliptic problems. Amsterdam: North-Holland; 1978.
[33] Brenner SC, Scott LR. The Mathematical Theory of Finite Element Methods. third ed. New York: Springer-Verlag; 2008.
[34] Glowinski R. Numerical methods for nonlinear variational problems. New York: Springer-Verlag; 1984.
[35] Alberty J, Carstensen C, Funken SA, R. Klose: Matlab implementation of the finite element method in elasticity. Computing 2002;69:239–63.